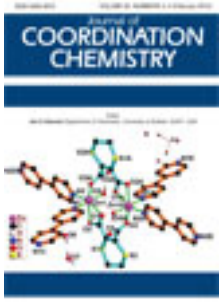

Journal of Coordination Chemistry
Publication details, including instructions for authors and subscription information:
http://www.tandfonline.com/loi/gcoo20

DNA-binding and cleavage activity of a new alkoxo and acetate-bridged dinuclear copper(II) complex

Yu Mei [a], Jing-Jing Zhou [a], Hong Zhou [a] & Zhi-Quan Pan [a]
[a] Key Laboratory for Green Chemical Process of Ministry of Education, Wuhan Institute of Technology, Wuhan 430073, P.R. China
Published online: 06 Feb 2012.

To cite this article: Yu Mei, Jing-Jing Zhou, Hong Zhou & Zhi-Quan Pan (2012) DNA-binding and cleavage activity of a new alkoxo and acetate-bridged dinuclear copper(II) complex, Journal of Coordination Chemistry, 65:4, 643-654, DOI: 10.1080/00958972.2012.658567

To link to this article: http://dx.doi.org/10.1080/00958972.2012.658567

Journal of Coordination Chemistry
Vol. 65, No. 4, 20 February 2012, 643–654

Taylor & Francis
Taylor & Francis Group

DNA-binding and cleavage activity of a new alkoxo and acetate-bridged dinuclear copper(II) complex

YU MEI, JING-JING ZHOU, HONG ZHOU* and ZHI-QUAN PAN*

Key Laboratory for Green Chemical Process of Ministry of Education,
Wuhan Institute of Technology, Wuhan 430073, P.R. China

(*Received 26 October 2011; in final form 19 December 2011*)

A new copper complex, $[Cu_2L(OAc)(CH_3OH)]\cdot CH_3OH$, where H_3L is 1,3-bis (5-methylsalicylideneimino)propan-2-ol, has been synthesized and characterized by single-crystal X-ray diffraction, IR, ES-MS, and UV-Vis techniques. The coordination polyhedra of copper(II) can be described as a tetrahedron and a planar quadrilateral. The interaction between the complex and calf thymus DNA/DNA was investigated by UV-Vis, fluorescence, circular dichroism spectra, and viscosity. All the results show that the interaction mode of the complex with DNA is intercalative with a binding constant of 1.16×10^5 $(\text{mol L}^{-1})^{-1}$ and linear Stern–Volmer quenching constant of 4.89×10^2 $(\text{mol L}^{-1})^{-1}$, respectively. Agarose gel electrophoresis exhibits that the complex can transform supercoiled to nicked form and exhibits effective DNA-cleavage activity *via* hydrolytic-cleavage mechanism.

Keywords: Crystal structure; DNA-cleavage activities; DNA-binding

1. Introduction

Study on natural phosphatase shows that highly effective hydrolysis activity of these enzymes depends on the active sites of the metal ions and noncovalent bonding with DNA [1]. To search for novel restriction enzymes and anticancer therapeutic agents, much effort has been made in synthesis and property investigation of mimics. Some transition metal complexes exhibit higher DNA-cleavage activities [2, 3]. These complexes can be bound to DNA in many noncovalent modes, such as ionic bonds, hydrogen bonds, π–π interactions, and hydrophobic interactions. The noncovalent interactions hold the complexes and DNA together, and enable binding of complexes and DNA, increasing cleavage activity of the complexes. Metal ions and the structures of the ligands in complexes are key factors to hydrolysis activities of the complexes [4–6].

Complexes derived from 1,3-bis(5-X-salicylideneimino)propan-2-ol ($X = Br$, Cl, and NO_2) have been structurally characterized and their magnetic properties determined [7–9]. However, the structure of this kind of complex with $X = CH_3$ has

*Corresponding authors. Email: hzhouh@126.com; zhiqpan@163.com

Journal of Coordination Chemistry
ISSN 0095-8972 print/ISSN 1029-0389 online
http://dx.doi.org/10.1080/00958972.2012.658567

not been reported. Herein, a dinuclear Cu(II) complex, $[Cu_2L(OAc)(CH_3OH)]\cdot CH_3OH$, ($H_3L = 1,3$-bis(5chlorosalicylideneamino)propan-2-ol) was synthesized and fully characterized. The complex is expected to interact with DNA *via* hydrogen-bonding and/or π–π interactions because of abundant donors and aromatic rings. These noncovalent interactions might promote DNA-cleavage activity by the complexes. Considering that no DNA-cleavage activity of this kind of complex has been investigated, this report will reveal for the first time the binding and cleavage with DNA.

2. Experimental

2.1. *Preparations*

5-Methylsalicylaldehyde was recrystallized from ethanol before use and other chemicals and solvents were of analytical grade and used as received. Calf thymus DNA (CT-DNA) was obtained from Sigma and used as received. 2-Hydroxy-1, 3-propanediamine was purchased from Alfa Aesar.

2.2. *Synthesis of complexes*

$[Cu_2L(OAc)(CH_3OH)]\cdot CH_3OH$: To solution of 5-methylsalicylaldehyde (0.136 g, 1 mmol) and 2-hydroxy-1,3-propanediamine (0.045 g, 0.5 mmol) in absolute methanol (15 mL), $Cu(OAc)_2\cdot 4H_2O$ (0.100 g, 1 mmol) in absolute methanol (10 mL) was added dropwise; the resulting solution was dark green. The mixture was stirred at room temperature for 5 h and then triethylamine (1 mL) was introduced. The resulting solution was stirred at ambient temperature for 24 h. After filtration, the resulting solution was allowed to evaporate slowly. The green block crystals suitable for X-ray measurement were collected. Yield: 0.145 g (80%). Anal. Calcd for $C_{23}H_{30}Cu_2N_2O_7$ (%): C, 48.16; H, 5.27; N, 4.88. Found: C, 48.53; H, 5.61; N, 4.64; IR (KBr, ν/cm^{-1}): 2915 ν(C–H), 1638 ν(C=N), 830 ν(C–H) (phenyl).

2.3. *Physical measurements*

IR spectra were measured using KBr discs on a Vector 22 FTIR spectrophotometer from 7500 to 370 cm^{-1}. Carbon, hydrogen, and nitrogen microanalyses were obtained on a Perkin-Elmer 240 analyzer. Electrospray mass spectra (ES-MS) were determined on a Finnigan LCQ ES-MS mass spectrograph using methanol as the mobile phase at 1.0 mmoldm^{-3}. Absorption spectra from 190 to 700 nm were recorded in a 1 cm pathlength quartz cuvette on a Shimadzu UV-2450 spectrophotometer. The scan times and spectral resolution are 4 and 1 cm^{-1} in IR, and 3 and 0.1 nm in UV measurements. Circular dichroic spectra of DNA were obtained using a Jasco J-810 spectropolarimeter. Fluorescence spectra were recorded on a Jasco FP-6500 spectrophotometer. Cyclic voltammograms were run on a CHI model 750 B electrochemical analyzer in DMF containing tetra(*n*-butyl)ammonium perchlorate (TBAP) as the supporting electrolyte. A three-electrode cell was used, which was equipped with a glassy carbon-working

electrode, a platinum wire as the counter electrode, and an Ag/AgCl electrode as the reference electrode. Scanning rates were 20–200 mV s^{-1}. The solution was deaerated for 15 min before measurements.

2.4. *X-ray data collection and refinement*

The crystals were measured on a Bruker AXS SMART diffractometer (Mo-Kα monochromator) [10]. The structures were solved by direct methods and refined by full-matrix least-squares based on F^2 [11]. Hydrogen atoms were located geometrically and refined in riding mode. The non-H atoms were refined with anisotropic displacement parameters. Calculations were performed using SHELX-97 crystallographic software package.

2.5. *DNA-cleavage experiment*

The cleavage of pBR322 DNA by the complex was examined by gel electrophoresis. Negative supercoiled pBR322 DNA (0.5 μg μL^{-1}) was treated with different concentrations of the complex (1 μL) in Tris-HCl buffer (1 μL, 50 mmol L^{-1} Tris-HCl, 50 mmol L^{-1} NaCl, pH = 7.2). After mixing, the DNA solutions were incubated at 37°C for 3 h. The reactions were quenched by addition of sterile solution (1 μL, 0.25% bromophenol blue, and 40% w/v sucrose). The samples were then analyzed by electrophoresis for 45 min at 116 V on agarose gel in TAE buffer (2.42 g Tris, 0.57 mL acetic acid and 0.372 g EDTA in 500 mL doubly distilled water, pH = 7.4, adjusted with HCl). The gel was stained with ethidium bromide (EB, 1 μg μL^{-1}) for 10 min after electrophoresis and then photographed.

3. Results and discussion

3.1. *Synthesis and characterization*

The complex was obtained by one-pot reaction between 5-methylsalicylaldehyde and 2-hydroxy-1,3-propanediamine in methanol solution containing copper(II) acetate, adjusted to weakly basic by adding triethylamine. The acetates and triethylamine form deprotoned ligand (L). The formation of the compound is evidenced by the presence of a strong IR band at 1638 cm^{-1}, due to C=N, while no bands *ca* 1680 as well as 3280 and 3350 cm^{-1}, corresponding to the absorption of C=O in 5-methylsalicylaldehyde and NH_2 in 2-hydroxy-1,3-propanediamine, respectively, have been detected [12].

3.2. *Electrospray mass spectra*

The ES-MS spectra of the complexes in acetonitrile solution are shown in figure 1. The peak at m/z 959.25, corresponding to $[Cu_4L_2(OAc)]^+$, is dominant and can be ascribed to the aggregation of the molecular unit $[Cu_2L(OAc)]$ and molecular ion unit $[CuL]^+$, confirming that the complex is stable in acetonitrile. This assignment is also confirmed by the isotope analysis of the peak. Good agreement between observed and calculated data is shown in the inset.

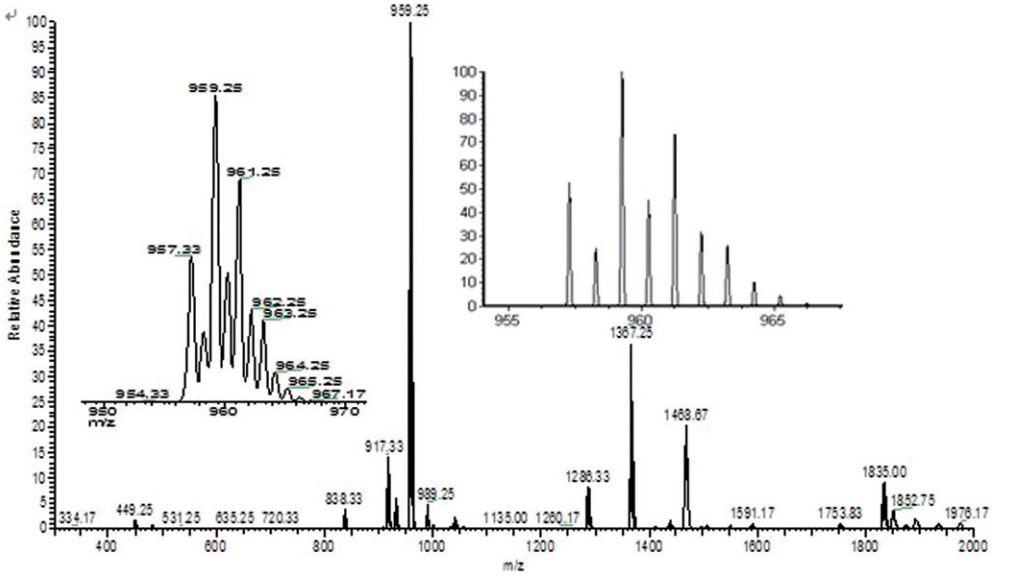

Figure 1. The ES-MS spectra of the complex (inset the isotopic distribution of the peak at $m/z = 959.25$; left: experimental pattern; right: calculated pattern).

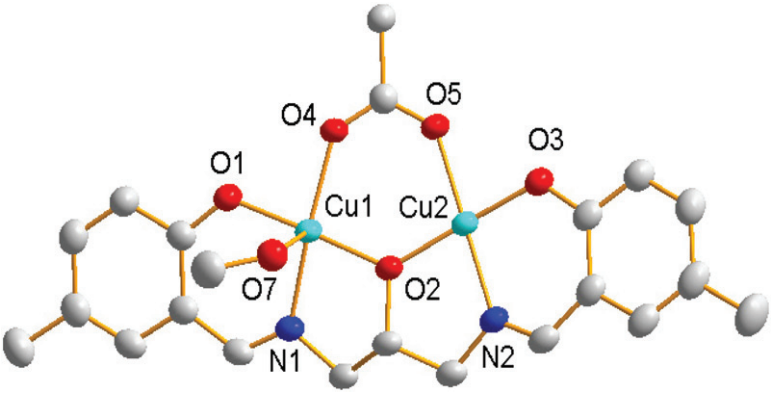

Figure 2. Perspective views of the $[Cu_2L(OAc)(CH_3OH)] \cdot CH_3OH$.

3.3. *Structure description*

The perspective view of $[Cu_2L(OAc)(CH_3OH)] \cdot CH_3OH$ is given in figure 2, together with the atom-numbering scheme. The crystallographic data and details about the data collection are presented in table 1. Selected bond lengths and angles relevant to the copper(II) coordination polyhedron are listed in table 2.

Table 1. Crystal data and structure refinement for the complex.

Empirical formula	$C_{23}H_{30}Cu_2N_2O_7$
Formula weight	573.57
Temperature (K)	291(2)
Crystal system	Monoclinic
Space group	*P21/n*
Unit cell dimensions (Å,°)	15.615(3)
a	
b	10.0403(18)
c	16.024(3)
α	90
β	101.299(2)
γ	90
Volume (Å^3), *Z*	2463.5(8), 4
Calculated density (g cm^{-3})	1.546
Absorption coefficient (Mo-Kα) (mm^{-1})	1.771
F(000)	1184
Crystal size (mm^3)	$0.22 \times 0.24 \times 0.28$
Mo-Kα radiation (Å^3)	0.71073
θ range for data collection (°)	2.4–26.0
Tot., unique data, *R*(int)	13,345, 4842, 0.022
$[I > 2\sigma\ (I)]$	$[S^2(F_o^2) + (0.06\,P)^2 + 1.99P]$
W^{-1}	$P = (F_o^2 + 2F_c^2)/3$
Observed data	3655
Nref, Npar	4842, 311
R, wR_2, *S*	0.0439, 0.1253, 1.05
Max. and av. shift/error	0.00, 0.00
Minimum and maximum resd. dens. (e Å^{-3})	−0.78 and 0.58

Table 2. Selected bond lengths (Å) and angles (°) for the complex.

Cu(1)–O(1)	1.892(3)	Cu(2)–O(2)	1.898(3)
Cu(1)–O(2)	1.913(3)	Cu(2)–O(3)	1.891(3)
Cu(1)–O(4)	1.962(3)	Cu(2)–O(5)	1.934(3)
Cu(1)–O(7)	2.580(3)	Cu(2)–N(2)	1.925(3)
Cu(1)–N(1)	1.936(3)		
O(1)–Cu(1)–O(2)	177.62(13)	O(1)–Cu(1)–O(4)	88.09(13)
O(1)–Cu(1)–O(7)	88.97(12)	O(1)–Cu(1)–N(1)	93.54(13)
O(2)–Cu(1)–O(4)	93.96(13)	O(2)–Cu(1)–O(7)	91.86(10)
O(2)–Cu(1)–N(1)	84.21(13)	O(4)–Cu(1)–O(7)	99.69(11)
O(4)–Cu(1)–N(1)	168.64(13)	O(7)–Cu(1)–N(1)	91.58(12)
O(2)–Cu(2)–O(3)	175.28(12)	O(2)–Cu(2)–O(5)	95.24(13)
O(2)–Cu(2)–N(2)	84.80(13)	O(3)–Cu(2)–O(5)	86.46(13)
O(3)–Cu(2)–N(2)	93.46(13)	O(5)–Cu(2)–N(2)	179.36(14)
Cu(1)–O(2)–Cu(2)	132.56(17)		

The molecular structure contains one L, two methanols, and one acetate. Two copper(II) ions are bridged by the alkoxo group of the ligand and by a μ_2-acetate. The Cu–Cu distance and Cu–O–Cu angle are 3.489 Å and 132.6°, respectively, close to counterparts in a similar complex [7]. The coordination polyhedra of copper(II) can be described as square pyramid for Cu(1) and square plane for Cu(2), respectively. The basal plane of Cu1 and the square plane of Cu2 are similar, composed of an imine, a phenolate, an acetate, and an alkoxo from one ligand. The distances between Cu and

coordination atoms are in the range 1.892–1.962 Å for Cu(1) and 1.891–1.934 Å for Cu(2). The apical position for Cu(1) is occupied by methanol with Cu–O distance of 2.580 Å.

As shown in figure 3, hydrogen-bonding interactions play an important role in maintaining the 3-D network. Each molecular unit is connected with four adjacent molecular units through hydrogen-bonding interactions, including O–H···O and C–H···O. For clarity, only one $[Cu_2L(OAc)(CH_3OH)]^+$ is shown in figure 3, while other adjacent four molecular units are omitted except for hydrogen-bonding interactions. The selected hydrogen-bonding parameters are O8–H8B···O3: $d_{O8-H8B} = 0.960$ Å, $d_{H8B\cdots O3} = 1.864$ Å, $d_{O8\cdots O3} = 2.823$ Å; O7–H7B···O8: $d_{O7-H7B} = 0.960$ Å, $d_{H7B\cdots O8} = 1.877$ Å, $d_{O7\cdots O8} = 2.737$ Å; C9–H9A···O1: $d_{C9-H9A} = 0.970$ Å, $d_{H9A\cdots O1} = 2.515$ Å, $d_{C9\cdots O1} = 3.431$ Å; C12–H12···O7: $d_{C12-H12} = 0.930$ Å, $d_{H12\cdots O7} = 2.484$ Å, $d_{C12\cdots O7} = 3.331$ Å. ∠O8–H8B···O3 = 176.7°, ∠O7–H7B···O8 = 148.0°, ∠C9–H9A···O1 = 157.4°, and ∠C12–H12···O7 = 151.5°.

3.4. *Absorption spectroscopic studies*

Absorption spectra of the complex in the absence and presence of CT-DNA at different concentrations (0–75 μmol L^{-1}) are shown in figure 4(a).

In the UV region, with increasing CT-DNA concentration for the complex, hypochromism in the band at 363 nm reaches as high as 22% with a blue shift. In order to quantitatively investigate the binding strength of the complex with CT-DNA, the intrinsic binding constant K_b was obtained by monitoring changes in absorbance at 360 nm for the complex as increasing concentration of CT-DNA using the equation $[DNA]/E_{ap} = [DNA]/E + 1/(K_bE)$, where $E_{ap} = \varepsilon_a - \varepsilon_f$, $E = \varepsilon_b - \varepsilon_f$; ε_a, ε_f, and ε_b correspond to $A_{obs}/[complex]$, the extinction coefficients for the free complex and the complex in the fully bound form, respectively. As shown in figure 4(b), K_b was

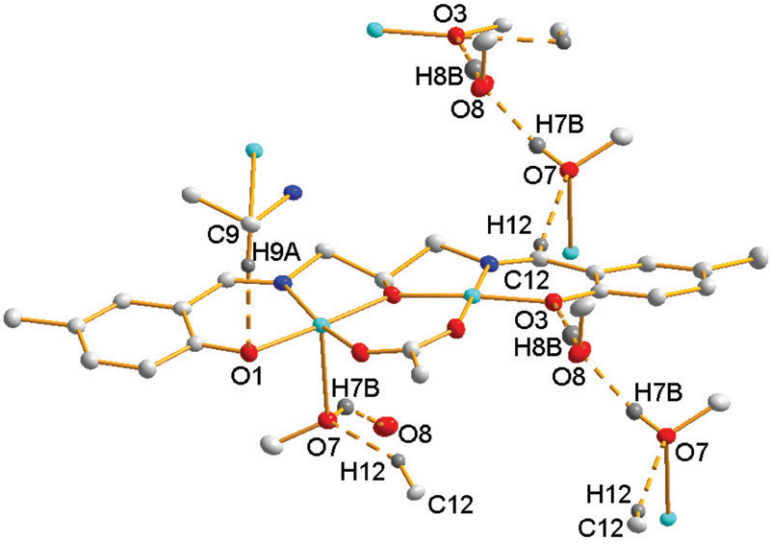

Figure 3. View of the hydrogen-bonding interactions of one molecular unit with adjacent ones.

1.16×10^5 $(\text{mol L}^{-1})^{-1}$ for complex calculated from the ratio of slope to the intercept from the plots of [DNA]/E_{ap} *versus* [DNA] [13]. The binding constant of K_b in the range 10^4–10^6 $(\text{mol L}^{-1})^{-1}$ fits to values of moderate intercalators. The intrinsic binding constant is higher than those of some dinuclear copper(II) complexes, μ-oxamido-bridged, and carboxylate-bridged copper(II) complex [14–16]. The better binding constant of the complex may be due to the better coplanarity of the complex, which is expected to have π–π stacking interactions between the base pairs in DNA and phenol rings in the complex [14, 17]. The large hypochromicity and the blue shift also illustrate intercalation between CT-DNA and the complex, likely through a stacking interaction between the aromatic chromophore in the complex and the base pairs of DNA [18–20].

3.5. *Fluorescence spectroscopic studies*

DNA solutions are not fluorescent and EB is weakly fluorescent, while solutions of DNA with EB show very strong fluorescence emission [21]. If Cu(II) complex added to the EB-DNA system replaces the bound EB, the emission intensity will be reduced. The emission spectra of EB bound to DNA in the absence and presence of Cu(II) complex are given in figure 5. It can be noted that the fluorescence intensity of the EB-DNA solutions decreases with the addition of Cu(II) complex, suggesting that the Cu(II) complex can replace EB and bind to DNA.

According to the classical Stern–Volmer equation $I_0/I = 1 + K[Q]$, in which I_0 and I are the fluorescence intensities in the absence and presence of complex, respectively, K is the linear Stern–Volmer quenching constant and $[Q]$ is the concentration of the complex, the relative binding propensity of the complexes to CT-DNA can be determined [22]. The fluorescence intensity at 607 nm ($\lambda_{ex} = 520$ nm) of EB in the bound form was plotted against the compound concentration. The quenching constants K obtained for complex are given by the slopes of the plots in figure 6. The K is 4.89×10^2 $(\text{mol L}^{-1})^{-1}$ for complex. The result demonstrates that Cu(II) complex can interact with DNA with moderate intercalation, similar to the absorption experiment.

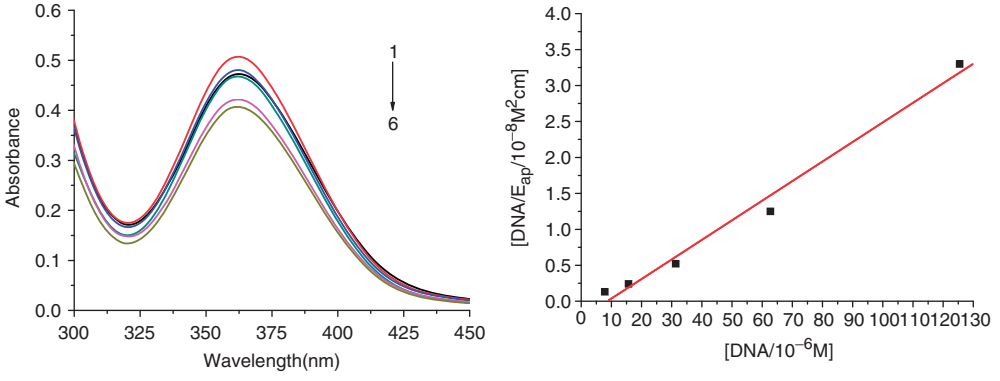

Figure 4. (a) Absorption spectra of the complexes in Tris-HCl buffer upon addition of CT-DNA; (b) plot of [DNA]/E_{ap} *vs.* [DNA] for absorption titration of CT-DNA with complex.

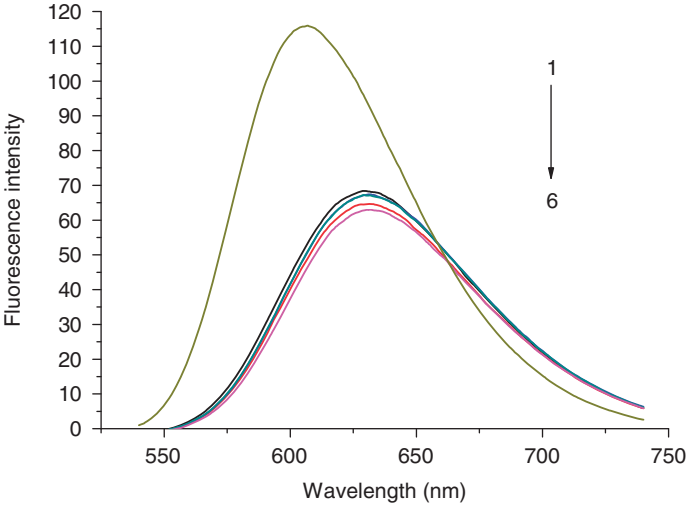

Figure 5. Emission spectra of EB bound to DNA in the absence (1) and presence (2–6) of Cu(II) complex. [EB] = 10 μmol L^{-1}, [DNA] = 25 μmol L^{-1}, [complex] 1–6 = 0, 25, 50, 100, 150, 200 μmol L^{-1}, respectively; λ_{ex} = 520 nm. The arrow shows the intensity changes on increasing complex concentration.

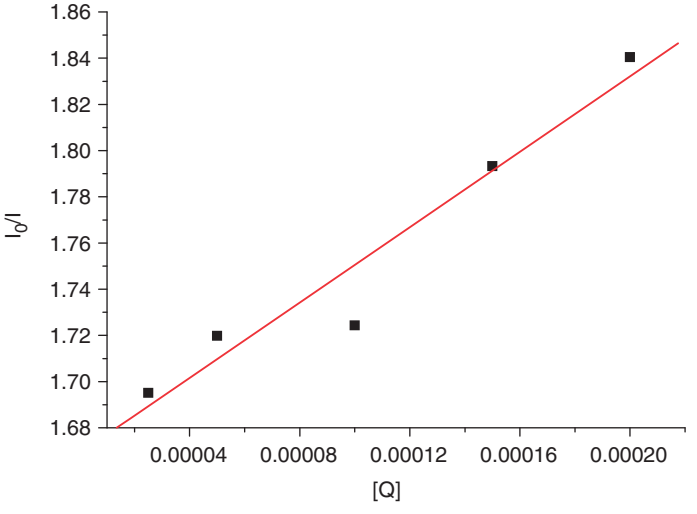

Figure 6. Stern–Volmer quenching plots of EB bound to DNA by Cu(II) complex. I_0 is emission intensity of EB-DNA in the absence of complex; I is emission intensity of EB-DNA in the presence of complex; [Q] = [complex].

3.6. *Circular dichroism spectra*

CT-DNA is present in the B-DNA form and shows a negative CD band at 245 nm caused by the helical conformation and a positive CD band at 275 nm due to base stacking [23]. The CD spectra of CT-DNA treated with Cu(II) complex with the ratio of 0.5 ([complex]/[DNA]) shows an evident disturbance on the CT-DNA conformation,

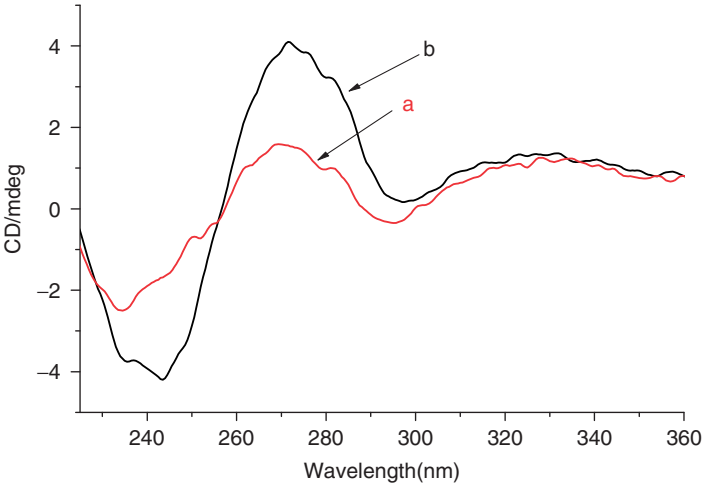

Figure 7. The circular dichroism spectra of CT-DNA in the absence (a) and presence of Cu(II) complex (b). [CT-DNA] = 25 μmol L^{-1}, [complex]/[DNA] = 0.5. All the spectra were recorded in Tris-HCl buffer, pH = 7.2.

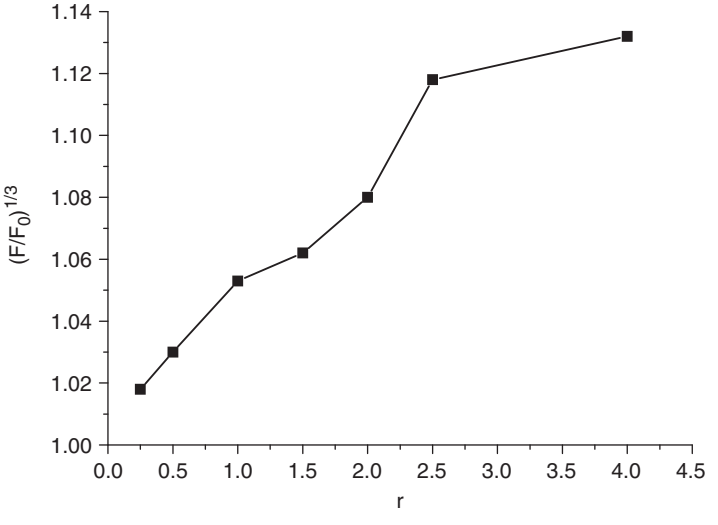

Figure 8. Effects of increasing amounts of Cu(II) complex on the relative viscosities of CT-DNA at 23 (±0.1)°C; [DNA] = 100 μmol L^{-1}, r = [M]/[DNA].

both positive and negative bands increase in intensity when adding Cu(II) complex to CT-DNA solution (figure 7). These data suggest that the Cu(II) complex can intercalate the DNA base pairs and unwind the DNA helix [24], and have stronger actions in latter.

3.7. *Viscosity study*

To further confirm the interaction mode of the copper complex with DNA, a viscosity study was carried out (figure 8). The specific viscosity contribution due to the DNA in

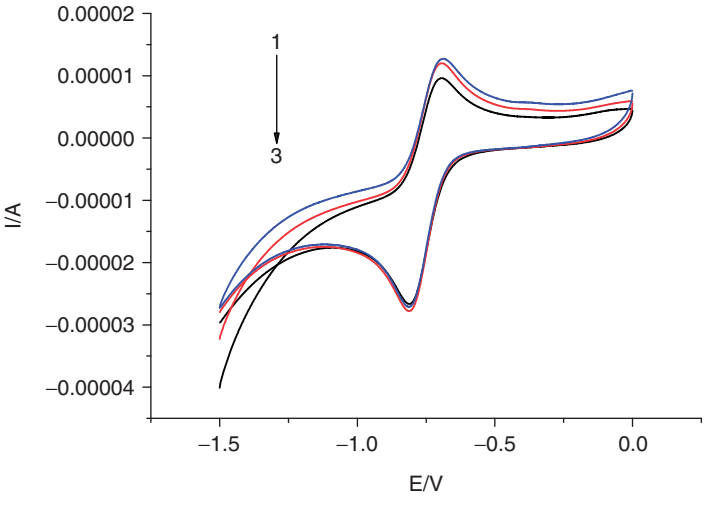

Figure 9. Cyclic voltammograms of the complex (1×10^{-4} mol L^{-1}) with different scan rates: 1–3 = 140, 120, 100 mVs^{-1}, in 50 mmol L^{-1} Tris-HCl/50 mmol L^{-1} NaCl buffer solution (pH = 7.2).

the presence of a binding agent was obtained. The results indicate that the presence of copper complex has a marked effect on the viscosity of DNA. The specific viscosity of DNA increases obviously with addition of increasing amounts of copper complex. The results illustrate that copper complex may intercalate between DNA base pairs [25, 26].

3.8. *Electrochemical studies*

Electrochemical properties of the complex were studied by cyclic voltammetry in 50 mmol L^{-1} Tris-HCl/50 mmol L^{-1} NaCl buffer solution (pH = 7.2) using tetrabutylammonium perchlorate (TBAP) as supporting electrolyte in the potential range −1.5 to 0 V. The cyclic voltammograms with different scan rates are shown in figure 9. The CV curve of the complex has a cathodic peak and an anodic peak with $E_{1/2} = -0.751$ V, $\Delta E = 0.101$ V, indicating a quasi-reversible process [27]. The larger negative potential ($E_{pc} = -0.70$ V at 100 mVs^{-1}) for the reduction peak reveals that the Cu(II) ions in the complex are not easy to be reduced in Tris-HCl buffer solution (pH = 7.2).

3.9. *DNA cleavage*

DNA-cleavage experiments were performed using a double stranded DNA plasmid. The metal complexes cause random nicks (cuts) to one of the DNA strands. As a consequence, the supercoiled form opens to form an open circular after one nick and subsequently to a linear form (linear DNA) if two nicks on complementary strands are within a short distance.

Finally, the DNA gets degraded into small pieces of different size which cannot be detected in our assay. The cleavage products were subjected to gel electrophoretic separation and the gels analyzed after EB staining.

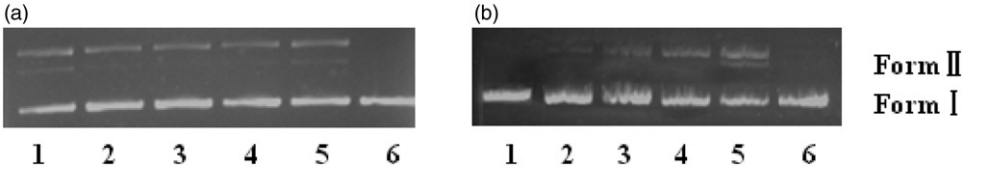

Figure 10. Gel electrophoresis diagram showing the cleavage of pBR322 DNA (0.5 μg μL^{-1}) by the complex in 50 mmol L^{-1} Tris-HCl/NaCl buffer (pH 7.2) at 37°C. (a) In different incubation time: Lane 1–5, DNA + complex (100 μmol L^{-1}) for 1 h, 2 h, 3 h, 4 h, 5 h, Lane 6, DNA control; (b) in different complex concentration (incubation time 3 h), Lanes 1–5, DNA + complex (12.5 μmol L^{-1}, 25 μmol L^{-1}, 50 μmol L^{-1}, 100 μmol L^{-1}, 200 μmol L^{-1}), respectively; Lane 6, DNA control.

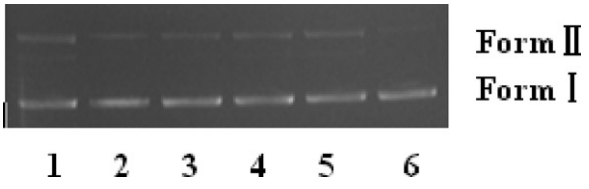

Figure 11. Gel electrophoresis diagram showing the cleavage of pBR322 DNA (0.5 μg μL^{-1}) by the complex with different scavenging agents in 50 mmol L^{-1} Tris-HCl/NaCl buffer (pH 7.2) and 37°C for 3 h: Lanes 1–4, DNA + complex (100 μmol L^{-1}) + 5 mmol L^{-1} EtOH; DMSO; KI; NaN_3. Lane 5, DNA + complex (100 μmol L^{-1}); Lane 6, DNA control.

The DNA-cleaving ability has been investigated with various concentrations and incubation times (figure 10). Incubation time has little effect on the cleavage activity, but with enhancement of concentration, the cleavage ability of the complex increases obviously. When the concentration of the complex is 200 μmol L^{-1}, the complex cleaves DNA into Form II (nicked form) and Form III (linear form).

To illuminate the DNA-cleavage mechanism by the complex, some scavenging agents, hydroxyl radical scavengers (5 mmol L^{-1} DMSO and 5 mmol L^{-1} EtOH), superoxide scavenger (5 mmol L^{-1} KI), and singlet oxygen scavenger (5 mmol L^{-1} NaN_3), were added in the incubation solution. The results of DNA cleavage in the presence or absence of scavenging agents are presented in figure 11. No obvious change of DNA-cleavage activity of the complex is observed, indicating that an oxidative cleavage is not responsible to the cleavage activity, which is in agreement with the CV results. Therefore, the DNA-cleavage activity is ascribed to hydrolytic cleavage.

4. Conclusion

A new alkoxo and acetate-bridged dinuclear copper(II) complex was obtained by [2 + 1] condensation of 5-methylsalicylaldehyde and 2-hydroxy-1,3-propanediamine in the presence of Cu^{2+}. The complex is stable in acetonitrile solution and Cu(II) ions in the complex are difficult to reduce due to the larger negative potential of the reduction peak. DNA-cleavage experiments with various scavenging agents show that the

complex exhibits effective DNA-cleavage activity *via* hydrolysis. The DNA-binding of the complex has been investigated by UV-Vis absorption, fluorescence, circular dichroism spectra, and viscosity. Results suggested that the complex binds to CT-DNA by intercalation and the binding constant of the complex is higher than those of μ-oxamido-bridged or carboxylate-bridged dicopper(II) complexes, perhaps from stronger π–π stacking interactions between phenol rings in the complex and the base pairs in DNA.

Acknowledgments

We are grateful to the National Nature Science Foundation of China (grant Nos. 20871097, 20971102, and 21171135) for the financial support.

References

[1] J.E. Deweese, F.P. Guengerich, A.B. Burgin. *Biochemistry*, **48**, 38 (2009).
[2] N. Raman, J.D. Raja. *J. Chem. Sci.*, **119**, 4 (2007).
[3] G. Fei, Y. Caixia, Y. Pin. *Chin. Sci. Bull.*, **49**, 16 (2004).
[4] F. Gago. *A Companion to Methods in Enzymol.*, **14**, 277 (1998).
[5] S.I. Kirin, C.M. Happel, S. Hrubanova, T. Weyhermuller. *Dalton Trans.*, 1201 (2004).
[6] C.L. Liu, S. Yu, D.F. Li, Z. Liao. *Inorg. Chem.*, **41**, 4 (2002).
[7] C.T. Zeyrek, A. Elmali, Y. Elerman, I. Svoboda, H. Fuess. *Chem. Sci.*, **50**, 11 (2000).
[8] E. Kavlakoglu, A. Elmali, Y. Elerman. *Phys. Sci.*, **57**, 5 (2002).
[9] V.V. Lukov, V.A. Kogan, V.M. Novotortsev, P.Yu. Tupolova, I.E. Gevorkyan. *Russ. J. Coord. Chem.*, **31**, 5 (2005).
[10] *SMART and SAINT, Area Detector Control and Integration Software*, Siemens Analytical X-Ray Systems, Inc., Madison, Wisconsin, USA (1996).
[11] G.M. Sheldrick. *SHELXTL V5.1 Software Reference Manual*, Bruker AXS, Inc., Madison, Wisconsin, USA (1997).
[12] H. Keypour, H. Khanmohammadi, K.P. Wainwright, M.R. Taylor. *Inorg. Chim. Acta*, **355**, 286 (2003).
[13] A.M. Pyle, J.P. Rehmann, C.V. Kumar. *J. Am. Chem. Soc.*, **111**, 3051 (1989).
[14] H.H. Lu, Y.T. Li, Z.Y. Wu, K. Zheng, C.Y. Yan. *J. Coord. Chem.*, **64**, 1360 (2011).
[15] S.H. Cui, M. Jiang, Y.T. Li, Z.Y. Wu, X.W. Li. *J. Coord. Chem.*, **64**, 4209 (2011).
[16] C. Gao, X. Ma, J. Lu, Z.G. Wang, J.L. Tian, S.P. Yan. *J. Coord. Chem.*, **64**, 2157 (2011).
[17] S. Anbu, M. Kandaswamy. *Polyhedron*, **30**, 123 (2011).
[18] J. Liu, T.B. Lu, H. Li. *Transition Met. Chem.*, **27**, 686 (2002).
[19] S. Wu, Z. Li, L. Ren, B. Chen, F. Liang, X. Zhou, T. Jia, X. Cao. *Bioorg. Med. Chem.*, **14**, 2956 (2006).
[20] J.L. Tian, L. Feng, W. Gu, G.J. Xu, S.P. Yan, D.Z. Liao, Z.H. Jiang, P. Cheng. *J. Inorg. Biochem.*, **101**, 196 (2007).
[21] F.J. Meyer-Almes, D. Porschke. *Biochemistry*, **32**, 16 (1993).
[22] J.B. LePecq, C. Paoletti. *J. Mol. Biol.*, **27**, 7 (1967).
[23] P.U. Maheswari, M. Palaniandavar. *J. Inorg. Biochem.*, **98**, 2 (2004).
[24] Y. Shao, X. Sheng, Y. Li, Z.L. Jia, J.J. Zhang, F. Liu, G.Y. Lu. *Bioconjugate Chem.*, **19**, 1840 (2008).
[25] J. Sun, S. Wu, Y. An, J. Liu, F. Gao, L.N. Ji, Z.W. Mao. *Polyhedron*, **27**, 13 (2008).
[26] J.G. Liu, B.H. Ye, H. Li, Q.X. Zhen, L.N. Ji, Y.H. Fu. *J. Inorg. Biochem.*, **76**, 3 (1999).
[27] J.A. Zhang, M. Pan, R. Yang, Z.G. She, W. Kaim, Z.J. Fan, C.Y. Su. *Polyhedron*, **29**, 1 (2010).